PHYSICAL REVIEW B

CONDENSED MATTER

THIRD SERIES, VOLUME 24, NUMBER 4 15 AUGUST 1981

Transition-metal impurities in CoGa

G. A. Benesh* and D. E. Ellis
Department of Physics and Astronomy, Northwestern University, Evanston, Illinois 60201
and Materials Research Center, Northwestern University, Evanston, Illinois 60201
(Received 22 January 1981)

Self-consistent embedded cluster models are developed to describe the electronic structure of CoGa, and of isolated transition-metal impurities (Ti,V,Cr) in CoGa. First-principles local-density theory is used in a variational linear combination of atomic orbitals framework to obtain effective charge and spin configurations of host and impurity atoms. 9, 15, and 27 atom clusters are considered; charge configurations are somewhat sensitive to cluster size, and spurious spin polarization of peripheral Co atoms is observed in the smaller clusters. The large-cluster results are consistent with experimental interpretations.

I. INTRODUCTION

CoGa is a type VIII—IIIA binary alloy that crystallizes in the $B2$ (CsCl) structure over a cobalt composition range of 45—65 at.%.[1] The stoichiometric, perfectly ordered compound is believed to be a very weak paramagnet. On the Co-rich side of stoichiometry, cobalt substitutes as antistructure (AS) atoms on the gallium lattice. However, when excess Ga is added, no similar substitution of gallium for cobalt occurs; instead, a defect structure is formed with vacancies on cobalt sites.[2]

Magnetization and magnetic susceptibility measurements of Co-Ga alloys over a wide range of composition have detected rather interesting magnetic properties, most of which can be attributed to the Co AS atoms. Mössbauer measurements on stoichiometric CoGa (Ref. 3) have revealed that structural Co atomic sites are nonmagnetic. Similar measurements on Co-rich alloys have shown that two inequivalent Co sites exist, one magnetic (presumably the AS site) and one nonmagnetic (structural Co). Booth and Marshall found that quenched CoGa alloys richer than 51 at. % cobalt were ferromagnetic.[4] Their determination of the Curie temperatures and intrinsic magnetizations of several Co-rich compounds correlated well with Co concentrations; hence, they associated the ferromagnetic properties with the formation of AS cobalt atoms. Susceptibility measurements[5–9] have revealed a Curie-Weiss law behavior at high temperatures ($\gtrsim$100 K). The measured Curie constants also correlated well with the AS concentration, and an effective magnetic moment of $\simeq 5\mu_B$ can be associated with each AS atom.[6,8,10] However, the effective magnetic moment decreases dramatically for AS concentrations below 2%.[6] This decrease could be attributed to the lack of clustered Co AS atoms below a critical concentration. Amamou and Gautier[7] studied the AS dependence of the magnetic moments and suggested that (i) isolated Co atoms on Ga sites are nonmagnetic, (ii) neighboring pairs of antistructure atoms are somewhat magnetic, and (iii) clusters of four Co atoms are strongly magnetic. Sellmyer and Kaplow[10] have similarly found that single AS atoms are nonmagnetic, and that clusters

of three or more AS atoms are highly magnetic, having effective magnetic moments of $5.7\mu_B$ per AS atom. The proposed clustering of Co AS atoms is consistent with the neutron diffraction and x-ray measurements of Booth and Pritchard[11] for $Co_2Ga_{2-x}Ti_x$ ($0 < x < 1$) alloys and small-angle diffuse neutron scattering data of Cywinski *et al.*[12] for Co-rich CoGa alloys. The latter report large superparamagnetic assemblies (> 20 Å) in quenched alloys; these large clusters were related to spin-correlated groups of AS cobalt atoms. Experimental resistivity measurements[13,14] in which high-temperature resistivity minima are observed are also consistent with a model in which giant spin clusters exist.

The introduction of transition metal (TM) impurities into CoGa produces effects that are similar to those caused by excess Co atoms. The compounds $Co_2Ga_{2-x}Ti_x$, $Co_2Ga_{2-x}V_x$, and $Co_2Ga_{2-x}Cr_x$ become ferromagnetically ordered for concentrations of $x \simeq 0.50$, 0.25, and 0.10, respectively.[11,15] Neutron scattering experiments on the Ti alloys reveal that the Ti atoms are nonmagnetic and that the cobalt atoms remain nonmagnetic until $x \gtrsim 0.50$.[11,16] For the V and Cr impurity alloys, neutron scattering indicates that some structural Co atoms become magnetic (possibly near impurity atoms), that V atoms are nonmagnetic, and that Cr atoms are magnetic.[17,18] Electrical resistivity measurements of $CoGa_{0.95}V_{0.05}$ and $CoGa_{0.95}Cr_{0.05}$ show that the V alloy is paramagnetic while the Cr alloy is superparamagnetic.[19] A low-temperature resistivity minimum is observed for each alloy, and the $\ln T$ temperature dependence may be associated with the formation of local moments.[19]

It has been well established both experimentally and theoretically that the magnetic state of a dilute transition-metal impurity in a metallic matrix depends mainly upon the local environment of the impurity. Additionally, in the case of an intermetallic compound the local environment seems to play an important role in the ferromagnetic properties of the compound. Thus, as the first step in the theoretical examination of impurities in CoGa, we have performed first-principles calculations on 9, 15, and 27 atom clusters representing CoGa sites and *isolated* impurity sites. Co_{15} clusters embedded in CoGa were studied to explore the ferromagnetic states resulting from cluster TM atoms. A further goal of this work is to test whether such cluster models can predict the presence or absence of magnetic moments in CoGa, and to examine the cluster-size dependence of such predictions.

II. THEORETICAL MODEL AND COMPUTATIONAL PROCEDURE

A. Exchange correlation

Our original study of CoGa (Ref. 20) utilized the spin-unrestricted Hartree-Fock-Slater (HFS) formalism.[21] The essential point of this theory is that the nonlocal Hartree-Fock exchange potential is approximated by a local, spin-dependent exchange potential. In Hartree atomic units this potential is of the form

$$V_{x\alpha}^{\sigma}(\vec{r}) = -3\alpha\left[\frac{3}{4\pi}\rho_{\sigma}(\vec{r})\right]^{1/3} , \tag{1}$$

where α is the exchange scaling parameter and ρ_σ is the electronic charge density of spin σ. In this work α was chosen as 0.70, close to the Kohn-Sham value of $\frac{2}{3}$ frequently used in metals calculations.

In our extended CoGa calculations on 15 and 27 atom clusters, correlation effects were more exactly included through a further local density approximation. Since both polarized and nonpolarized calculations of similar clusters were made, it was desirable to use an exchange-correlation potential that could be easily adapted to either model. For these reasons, the Gunnarsson-Lundqvist potential[22] was adopted. It can be written as

$$V_{xc}^{\pm}(\vec{r}) = V_x(\vec{r})[\beta(r_s) \pm \tfrac{1}{3}\delta(r_s)\zeta/(1 \pm \gamma\zeta)] , \tag{2a}$$

where

$$\beta(r_s) = 1 + 0.0545 r_s \ln(1 + 11.4/r_s) , \tag{2b}$$

$$\delta(r_s) = 1 - 0.036 r_s - 1.36 r_s/(1 + 10 r_s) , \tag{2c}$$

$$V_x(\vec{r}) = -2\left[\frac{3}{8\pi}\rho(\vec{r})\right]^{1/3} , \tag{2d}$$

$$r_s(\vec{r}) = \left[\frac{3}{4\pi}\right]^{1/3}\rho(\vec{r})^{-1/3} , \tag{2e}$$

$\gamma = 0.297$, and ζ is the fractional magnetization $(\rho_+ - \rho_-)/\rho$. The (+) and (−) denote spin-up and spin-down terms, respectively. For the nonpolarized calculations the second term in square brackets in Eq. (2a) was omitted.

B. Self-consistency procedure

Molecular-orbital energies and wave functions were obtained by a discrete-variational method described previously.[23,24] Eigenfunctions were expanded as a linear combination of symmetry orbitals which were themselves expanded as a linear combination of atomic orbitals (LCAO) centered on

the different cluster atoms. The matrix secular equation $(H-ES)C=0$ was solved by standard procedures and Fermi-Dirac statistics were invoked to determine occupation numbers f_i for each molecular orbital (MO).[25] The *cluster* charge density was then constructed by summing over all MO's:

$$\rho_{\text{cluster}} = \sum f_i \,|\, \psi_i(\vec{r}) \,|^2 \ . \tag{3}$$

This charge density was approximately decomposed by Mulliken populations as

$$\rho_{\text{cluster}} \approx \sum_{\nu nl} f_{nl}^{\nu} \,|\, R_{nl}(r_\nu) \,|^2 \ , \tag{4}$$

where f_{nl}^{ν} denotes the occupation of the nl atomic shell of atom ν.

For bulklike clusters, the *crystal* charge density was constructed for the next self-consistent (SC) cycle by extending the sum over atoms in Eq. (4) to infinity and averaging with previous cycles. A previously described one-parameter pseudopotential[26] was used to truncate exterior wells to prevent electron transfer from the cluster into filled exterior states. Clusters representing dilute transition-metal (TM) impurities in CoGa were embedded in the SC potential of the pure solid. Since the crystal potential is that of the unperturbed, nonmagnetic alloy, TM impurity effects were limited to nearest-neighbor, second-neighbor, and third-neighbor shells in the 9-, 15- and 27-atom clusters, respectively. It should be emphasized that these calculations are for *isolated* impurity atoms. Impurity-impurity interactions have not been included in this study.

C. Basis sets

The atomic orbitals used in the molecular-orbital expansion were obtained by solving the self-consistent free-atom problem. Several numerical free-atom basis sets were considered in these calculations. Because the Mulliken population analysis is often misleading when describing rather diffuse charge,[27] it is desirable to restrict the spatial extent of some valence and unoccupied atomic levels. Thus, the Mulliken population of a valence Co orbital could then more reasonably be associated with a Co atom. Also, the reduced overlap between orbitals on different atomic sites produces an improved variational basis. The limited spatial extent of valence orbitals, however, should not be so great as to significantly affect the atomic core orbitals. Spherical wells of varying depth and radial extent were added to the atomic potentials so that different basis sets could be constructed. The set obtained by adding a well of depth 4 a.u. and radius 5 a.u. best satisfied the criteria listed above. This basis consisted of Co, Ga, and TM $1s$, $2s$, $2p$, $3s$, $3p$, $3d$, $4s$, and $4p$ orbitals. In the early calculations, Ga $5s$, $5p$ and Co $4d$, $5s$, $5p$ orbitals were added to increase the variational freedom. However, the low population of these levels indicated that they were probably not needed, so in subsequent calculations on larger clusters they were omitted.

TABLE I. Self-consistent atomic-orbital populations for bulklike CoGa clusters.

Orbital	$GaCo_8(sp)$[a]	$GaCo_8(np)$[b]	$CoGa_8(sp)$	$CoGa_8(np)$	Crystal potential
Ga $3d$	9.99	9.98	10.00	10.00	10.00
$4s$	0.80	1.23	1.81	1.63	0.80
$4p$	1.13	1.02	0.77	1.02	1.12
$5s$	0.20	0.08	0.03	0.05	0.20
$5p$	0.41	0.10	0.02	0.06	0.40
Co $3d$	7.53	7.33	7.41	7.32	7.68
$4s$	1.06	1.25	0.88	0.99	1.00
$4p$	0.51	0.64	0.40	0.53	0.46
$4d$	0.28	0.16	0.85	0.11	0.28
$5s$	0.04	0.04	0.04	0.04	0.04
$5p$	0.02	0.02	0.07	0.04	0.02

[a]Denotes spin-polarized calculation.
[b]Denotes nonpolarized calculation.

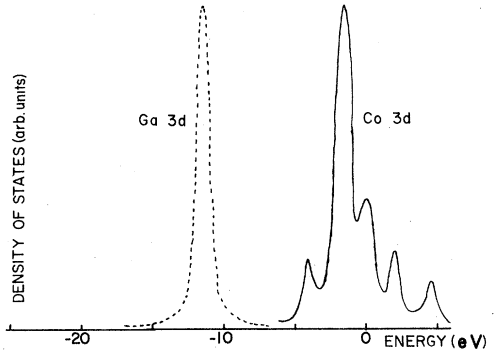

FIG. 1. Partial density of states for $CoGa_8$ cluster; Co $3d$ (solid curve) and Ga $3d$ (dashed).

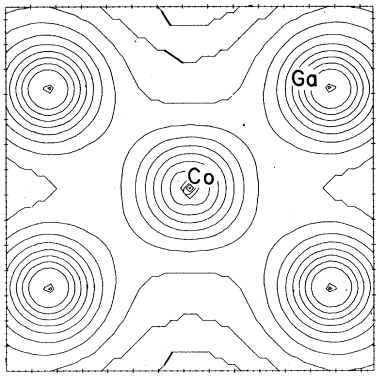

FIG. 2. Self-consistent valence charge density in $CoGa_8$ cluster. Logarithmic contour levels are 6.70, 3.35, 1.68,. . .e/a_0^3.

III. RESULTS

A. Nine-atom impurity clusters

The self-consistent bulk CoGa crystal potential was chosen by considering the results from calculations on four bulklike clusters. In Table I, the final Mulliken populations for spin-polarized (sp) and nonpolarized (np) $GaCo_8$ and $CoGa_8$ clusters are listed. In each case the Co and Ga atomic-orbital populations were used to generate the crystal embedding potential. The number of electrons assigned to the AB_8 clusters was determined by the effective atomic charges as part of the self-consistency loop. The tabulated results give a reasonable picture, showing that the filled deep-lying Ga $3d$ band is not perturbed while ~ 0.5 electron is transferred from the valence shells onto cobalt sites. The Co $3d$ population is increased relative to the free-atom value of 7.0, as would be expected. Thus the minimal cluster results agree on the general features of the charge configuration; however, with noticeable site- and spin-dependent differences.

A typical partial density of states (PDOS) diagram, obtained for the $CoGa_8$ cluster, is shown in Fig. 1. Continuous curves are obtained by broadening the discrete cluster levels with a Lorentzian of width 0.4 eV. The Ga $3d$ band is seen to lie ~ 11 eV below the Fermi energy and is essentially decoupled from the partially occupied Co $3d$ band. The valence charge density, taken through a Ga-Co-Ga plane, is presented in the contour-level diagram of Fig. 2. The spin-polarized $GaCo_8$ cluster results were favored in choosing the crystal configuration for later calculations (last column of Table I) since the environment of this cluster most resembles that of the $(TM)Co_8$ clusters that are of interest. Table I also reveals the extremely small populations of the Co $5s$ and $5p$ atomic orbitals, indicating that their

TABLE II. Self-consistent atomic-orbital populations for MCo_8 clusters embedded in CoGa.

Orbital		M = Ti		V		Cr		Co		Ga	
M	$3d$	2.66[a]	0.08[b]	3.59[a]	1.13[b]	5.05[a]	2.11[b]	7.66[a]	1.50[b]	9.99[a]	0.01[b]
	$4s$	1.43	0.01	1.42	0.04	1.33	0.03	1.14	0.02	0.85	0.07
	$4p$	0.14	0	0.38	0.04	0.28	0.06	0.44		1.09	−0.07
Net spin			0.09		1.21		2.20		1.52		0.01
Co	$3d$	7.60	1.82	7.58	1.86	7.59	1.87	7.51	2.05	7.56	1.56
	$4s$	1.13	0.13	1.14	0.04	1.10	0.02	1.05	0.01	1.16	0.08
	$4p$	0.28	0.02	0.27	0.01	0.27	−0.01	0.34	−0.04	0.41	−0.01
Net spin			1.97		1.91		1.86		2.02		1.63

[a]Net population, ↑ + ↓ occupation.
[b]Net spin density, ↑ − ↓ occupation.

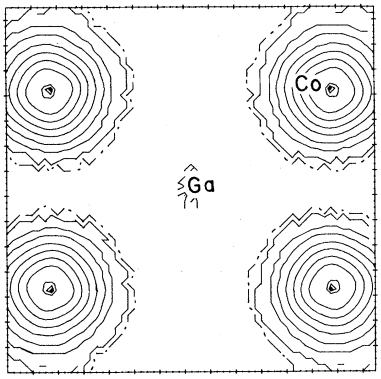

FIG. 3. "Spin halo" found in $GaCo_8$ clusters; spin density on log scale of ± 6.70, ± 3.35, ± 1.68,. . .e/a_0^3.

inclusion is not required for a basis to have sufficient variational freedom.

Self-consistent spin-polarized calculations were performed on MCo_8 clusters for M = Ga, Co, Ti, V, and Cr, representing a bulk gallium site, an antistructure cobalt site, and three impurity sites, respectively. The results for these clusters are compared in Table II. It can be seen that of the M atoms, the largest moments belong to the Cr, Co, and V atoms with substantially smaller moments ($< 0.1\mu_B$) on the Ti and Ga sites. The relative size of the magnetic moments $\mu_{Cr} > \mu_V > \mu_{Ti}$ is consistent with both the neutron scattering experiments and the relative impurity concentrations required for ferromagnetic ordering. The neighboring Co atoms are seen to have rather large magnetic moments ($\sim 2\mu_B$), not only in the vicinity of the impurity and AS atoms but also near the structural Ga atom.

The latter result, polarized Co atoms in a bulklike CoGa cluster (see Fig. 3), does not speak well for the present nine-atom cluster model. Experimental

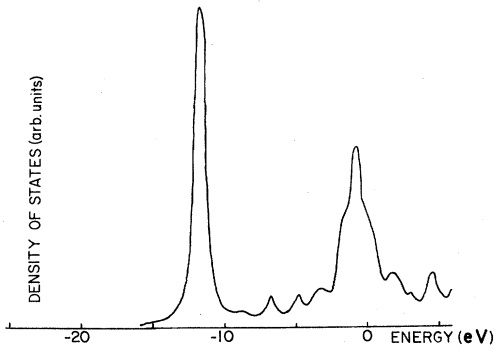

FIG. 4. Total density of states for CoGa using $CoGa_8Co_6$ cluster.

results rather strongly suggest that structural Co atoms are nonmagnetic, but our calculations describe a nearest-neighbor Co atom with an almost free-atom spin configuration. When a spin-polarized calculation was performed on a $CoGa_8$ cluster, the polarization of the $3d$ level was reduced to a value of only $0.12\mu_B$ (compared with $1.56\mu_B$ in the $GaCo_8$ cluster), a value much more consistent with experiment. Thus, the problem with the nine-atom cluster model appears to be in its description of the local environment of the *peripheral* cluster atoms. In the MCo_8 clusters, the Co atoms are rather isolated in the sense that only one nearest-neighbor atom (M) is explicitly included in the cluster wave function, the other nearest neighbors being approximated in the (spin-independent) crystal potential. Because of this relative isolation, the Co atoms develop a high-spin configuration that approaches that of the free atom. The atomic charge configuration, on the other hand, is already rather well determined by the embedded minimal cluster.

By expanding the size of the cluster to include in the cluster wave function some of the near neighbors to the peripheral Co atoms, one can obtain a more reliable model. We have thus performed first-principles calculations on 15 and 27 atom clusters which include four and seven of the eight Co near neighbors, respectively.

B. 15 and 27 atom impurity clusters

In order to obtain a crystal potential that more closely resembles the environment of an MCo_8Ga_6 cluster, a self-consistent calculation of a *nonpolarized* $GaCo_8Ga_6$ cluster was performed using smaller ($3d$,$4s$,$4p$) basis sets. This cluster was self-consistently embedded in its own crystal potential as described in Sec. II B. A nonpolarized calculation was performed so as to minimize the spin-dependent effects of the cluster boundary conditions (see preceding section). However, since the derived crystal potential was to be used in spin-polarized calculations, an exchange-correlation potential that could easily be made spin dependent was desired. For this reason, the potential of Gunnarsson and Lundqvist [Eq. (2)] was employed. The atomic populations found in this manner were Ga $3d(9.98)$ $4s(1.47)$ $4p(1.58)$ and Co $3d(7.21)4s(0.89)4p(0.88)$, with an indicated small charge transfer of 0.03 electrons from Co to Ga sites. The differences between this configuration and the $GaCo_8$ results listed in column 2 of Table I are due to three factors: (i) Interactions are treated more explicitly due to increased cluster size, (ii) reduced variational freedom

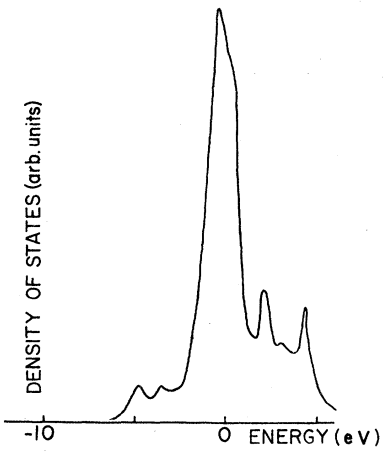

FIG 5. Central Co atom 3*d* partial density of states from $CoGa_8Co_6$ cluster.

of the smaller basis alters the charge transfer, and (iii) a somewhat different exchange-correlation potential was used. The resulting crystalline Coulomb and exchange-correlation potentials are very similar in the two models. In order to estimate the influence of factors (ii) and (iii) we recalculated several AB_8 clusters using the smaller basis sets, varying the assumed crystal atomic configurations, and comparing results of spin-polarized, Gunnarsson-Lundqvist, and von Barth-Hedin[28] exchange-correlation potentials. Only small quantitative changes in self-consistent atomic configurations and spin moments were observed in the results. This lack of sensitivity to theoretical and computational details allows us to interpret cluster size effects with some confidence.

In Fig. 4 we present a typical result for the total valence density of states of CoGa, using the $CoGa_8Co_6$ cluster result. In addition to the Co 3*d* band and the nearly isolated Ga 3*d* levels, one can see the metal *sp* contributions which extend across the entire energy range. A comparison of Fig. 5 with Fig. 1 shows that the central Co PDOS is only slightly modified by the addition of the Co_6 shell; the embedding potential is fairly effective in preserving this feature.

Self-consistent spin-polarized calculations were then performed on MCo_8Ga_6 clusters for M = Ga, Co, Ti, V, and Cr. The results from these calculations were very similar to the corresponding nine-atom cluster results. The eight Co atoms again polarized in all cases, including the bulklike $GaCo_8Ga_6$ cluster. The size of the Co magnetic moments is again $\sim 2\mu_B$ for all cases. When a spin-polarized calculation was performed on the cobalt-centered $CoGa_8Co_6$ cluster, the polarization of the central-atom 3*d* atomic level was reduced by more than a factor of 10, in analogy with the nine-atom cluster case. The same conclusions seem to apply to both the nine- and 15-atom clusters: The description of the local environment of the off-

TABLE III. Self-consistent atomic-orbital populations for $MCo_8Ga_6Ga_{12}$ clusters embedded in CoGa.

Orbital		M = Ti		V		Cr		Co		Ga	
M	3*d*	2.43[b]	0.002[b]	3.36[a]	0.004[b]	4.77[a]	0.008[b]	7.35[a]	0.010[b]	9.98[a]	0.003[b]
	4*s*	0.52	−0.001	0.59	−0.001	0.64	−0.001	0.72	−0.001	1.26	0
	4*p*	0.82	−0.001	0.93	−0.001	0.91	−0.001	1.03	−0.001	1.86	−0.001
Net spin			0		0.002		0.006		0.008		0.002
Co	3*d*	7.29	0.020	7.28	0.020	7.27	0.021	7.27	0.021	7.29	0.021
	4*s*	0.63	0.001	0.62	0.001	0.58		0.62	0.001	0.65	0.001
	4*p*	0.77		0.77		0.76		0.75		0.71	0
Net spin			0.021		0.021		0.021		0.022		0.022
Ga	3*d*	9.98	0	9.98	0	9.98	0	9.98	0	9.98	0
	4*s*	1.53	0	1.53	0	1.53	0	1.54	0	1.54	0
	4*p*	1.62	0	1.62	0	1.62	0	1.62	0	1.62	0
Net spin			0		0		0		0		0
Ga	3*d*	9.99	0	9.99	0	9.98	0	9.99	0	9.99	0
	4*s*	1.72	0	1.72	0	1.73	0	1.73	0	1.72	0
	4*p*	1.63	0	1.64	0	1.65	0	1.64	0	1.64	0
Net spin			0		0		0		0		0

[a]Net population, ↑ + ↓ occupation.
[b]Net spin density, ↑ − ↓ occupation.

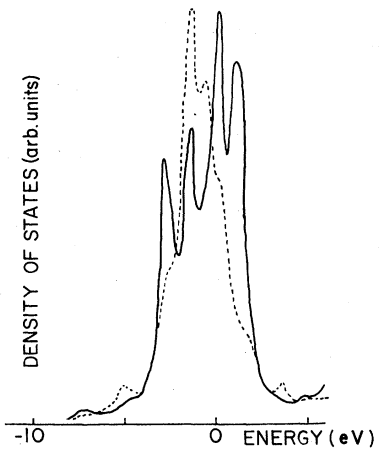

FIG 6. Cobalt 3*d* partial density of states using $CoCo_8Ga_6Ga_{12}$ cluster; central atom (solid curve) and first-neighbor shell (dashed).

center Co atoms is not yet well approximated as concerns the magnetic configuration.

The 27-atom clusters explicitly included seven of the eight nearest neighbors to the off-center cobalt atoms. The addition of this next shell of neighboring atoms had a dramatic effect on the Mulliken spin populations of the inner atoms, as can be seen in Table III. The magnetic moments of the eight cobalt atoms in the bulklike $GaCo_8Ga_6Ga_{12}$ cluster are reduced by a factor of about 100 when compared with either the 15- or 9-atom cluster results. The size of the cobalt moment in the $GaCo_8Ga_6Ga_{12}$ cluster can also be compared with that of the central Co in a bulklike $CoGa_8Co_6$ cluster in which the outer cobalts are constrained to be nonpolarized. These small Co moments of 0.02 and $0.01\mu_B$ agree well enough to indicate that the approximation of the local environment of the off-center Co atoms has been substantially improved. The resulting Co configuration 3*d*(7.29)4*s*(0.65) 4*p*(0.71) shows essentially the same number of *d* electrons as in the 15-atom cluster, the major change being an increased transfer of 4*s*,*p* electrons to the corresponding Ga levels. The net result is a charge transfer of 0.35 electrons from Co, primarily into diffuse levels of third- and fourth-shell Ga atoms.

The cluster results of Table III can also be compared with the experimental results outlined in the Introduction. On the basis of these calculations, we predict that isolated cobalt AS atoms are nonmagnetic and that isolated Ti, V, and Cr impurities on gallium sites are nonmagnetic as well. These conclusions agree well with the experimental interpretations in Refs. 6, 7, 9, 11, 12, and 15. In addition, we find that the moments on the central sites are very sensitive to the presence of magnetic moments on neighboring sites. This was especially evident in the 15-atom-cluster calculations.

The central-atom Co 3*d* and Co_8 neighbor shell 3*d* partial density of states for the Co AS cluster $CoCo_8Ga_6Ga_{12}$ are shown in Fig. 6. The two subbands display about the same width and position relative to E_F, but with different shapes. The peripheral Co_8 band is noticeably broadened in comparison with the corresponding 9- or 15-member clusters. This broadening is another manifestation of the Co—Ga bonding interaction which is apparently essential for determining the presence or absence of a moment.

C. Cobalt clusters in CoGa

The neutron data of Cywinski *et al.*[12] indicate a critical concentration of 55 at. % Co for the onset of ferromagnetism in quenched alloys (correcting the earlier result[4] of 51 at. %). At this concentration and higher, both superparamagnetism and ferromagnetism coexist. As an example of a possible

TABLE IV. Self-consistent atomic-orbital populations for $CoCo_8Co_6$ clusters embedded in CoGa.

	Central atom		Co_8 shell		Co_6 shell	
Orbital	Charge	Spin				
3*d*	7.29	1.85	7.17	2.20	7.08	2.30
4*s*	0.50	−0.03	1.24	0.01	1.04	0.04
4*p*	0.59	−0.004	1.02	−0.13	0.41	−0.01
net	+ 0.62	1.82	−0.43	2.08	+ 0.47	2.33

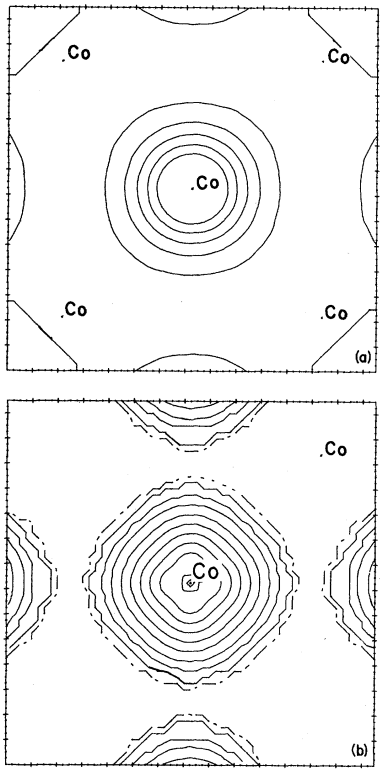

FIG. 7. Valence charge density (a) and spin density (b) for $CoCo_8Co_6$ cluster in CoGa in the (001) plane. Log contour levels are ± 0.84, ± 0.42, ± 0.21,. . . e/a_0^3. Atom positions above and below the basal plane are marked; dashed line in (b) denotes zero-spin contour.

ferromagnetic structure, we have considered a cubic cluster of 15 Co atoms embedded in CoGa. The self-consistent results indeed indicate ferromagnetic ordering, with the configuration indicated in Table IV. The valence charge density [Fig. 7(a)] is quite spherical, with an extended "free-electron-like" interstitial region. The spin density [Fig. 7(b)] exhibits a pronounced cubic component; in the interstitial region a weak negative 4*sp* polarization is found. These features are in general accord with our understanding of ferromagnetic transition metals.

In order to consider the probable clustered AS atom interactions postulated[12] for the large superparamagnetic assemblies, it will be necessary to treat larger clusters, of lower symmetry, than those considered in the present work. However, it is possible that an implicit scheme, by which the influence of neighboring AS moments is felt through a magnetic term in the embedding potential, could represent the essential interactions.

IV. CONCLUSIONS

Self-consistent calculations of 9- and 15-atom clusters representing Co AS and TM-impurity sites proved that these clusters inadequately described the magnetic behavior of these sites in CoGa. The inadequacy of the cluster model with regard to magnetic configuration was attributed to an incomplete description of the local environment of off-center cobalt atoms. The problem was reduced by adding a new shell of atoms so that seven of the eight nearest neighbors of these Co atoms were explicitly included in the cluster wave functions. We have previously found[26,27] that a simple embedding procedure, using cluster charge densities to synthesize the crystalline environment, greatly aids in determining spectral densities and charge configurations which are rather insensitive to cluster size or composition (e.g., $NiAl_8$ versus $AlNi_8$ in NiAl). The multiple scattering $X\sigma$ calculations of Johnson *et al.* for TM impurities in copper utilized 19-atom clusters, with isolated molecule boundary conditions.[29] Our results suggest that derived magnetic properties may be more sensitive to cluster size and boundary conditions that was assumed.

The KKR Green's-function method used by Podloucky *et al.* to calculate the electronic structure of TM impurities in Cu and Ag (Ref. 30) includes interactions with the complete crystal lattice. One has to carry out the self-consistent Green's-function calculation for the unperturbed lattice as an initial step. This may prove to be too difficult for complex (or disordered) lattices but is clearly worthwhile for "classic" systems like Cu and Pd. Unfortunately, numerical applications have not yet progressed beyond the single-site perturbation model. The extension to a perturbed cluster scheme would allow description of neighbor polarization and orbital delocalization effects, such as have been discussed in the present work.

The predicted magnetic properties of the CoGa system turn out to be a sensitive function of cluster size. This is interesting, since the difference between, for example, 15- and 27-atom clusters is not in the number of atoms included in the potential field, but instead in the orbital delocalization which the wave functions of larger clusters permit. Some experimentation with the potential embedding procedure suggests that it will not be easy to mimic these effects in small clusters. We may also apply wave-function boundary conditions which enforce delocalization and induce a pseudoband-structure model for the metal.[31] Further numerical experi-

ments will be helpful in determining parametrizations of boundary conditions and embedding potential which can better reproduce magnetic structure of extended systems. Results for the 27-atom clusters indicate that isolated AS atoms and isolated impurity atoms on gallium sites are nonmagnetic, in agreement with experiment. Co_{15} clusters were found to be ferromagnetic.

ACKNOWLEDGMENTS

This research was supported under the NSF-MRL program through the Materials Research Center of Northwestern University (Grant No. DMR 79-23573) and the Air Force Office of Scientific Research (Grant No. 81-0024).

*Current address: Cavendish Laboratory, University of Cambridge, Cambridge, CB3 OHE, England.

[1]K. Schubert, H. L. Lucas, H. G. Meissner, and S. Bhan, Z. Metallkde. 50, 534 (1959).
[2]A. Bradley and A. Taylor, Proc. R. Soc. London Sect. A 159, 56 (1937).
[3]K. R. P. M. Rao and P. K. Iyengar, Phys. Status Solidi A 30, 397 (1975).
[4]J. G. Booth and J. D. Marshall, Phys. Lett. A 32, 149 (1970).
[5]T. Goto, M. Ohashi, and K. Kamigaki, J. Phys. Soc. Jpn. 26, 207 (1969).
[6]E. Wachtel, V. Linse, and V. Gerold, J. Phys. Chem. Solids 34, 1461 (1973).
[7]A. Amamou and F. Gautier, J. Phys. F 4, 563 (1974).
[8]D. Berner, G. Geibel, V. Gerold, and E. Wachtel, J. Phys. Chem. Solids 36, 221 (1975).
[9]M. W. Meisel, W. P. Halperin, Y. Ochiai, and J. O. Brittain, J. Phys. F 10, L105 (1980).
[10]D. J. Sellmyer and R. Kaplow, Phys. Lett. A 36, 349 (1971).
[11]J. G. Booth and R. G. Pritchard, J. Phys. F 5, 347 (1975).
[12]R. Cywinski, J. G. Booth, and B. D. Rainford, J. Phys. F 7, 2567 (1977).
[13]T. Aoki, Y. Yamaguchi, and J. O. Brittain, *Proceedings of the 12th International Conference on Low Temperature Physics, Kyoto* (Science Council, Japan, 1970), p. 763; T. Aoki, thesis, Northwestern University, 1970.
[14]Y. Ochiai and J. O. Brittain, Phys. Lett A 73, 347 (1979).
[15]R. Cywinski and J. G. Booth, J. Phys. F 6, L75 (1976).
[16]P. J. Webster and K. R. A. Ziebeck, J. Phys. Chem. Solids 34, 1647 (1973).
[17]K. Raj, J. I. Budnick, T. J. Burch, R. Cywinski, and J. G. Booth, Physica 86–88B, 407 (1977).
[18]R. Cywinski and J. G. Booth, J. Phys. F 7, 1531 (1977).
[19]R. Cywinski, J. Phys. F 9, L29 (1979).
[20]G. A. Benesh and D. E. Ellis, Bull. Am. Phys. Soc. 25, 46 (1980); J. Appl. Phys. 52, 1676 (1981).
[21]J. C. Slater, *The Self-Consistent Field for Molecules and Solids* (McGraw-Hill, New York, 1974).
[22]O. Gunnarsson and B. I. Lundqvist, Phys. Rev. B 13, 4274 (1976).
[23]D. E. Ellis and G. S. Painter, Phys. Rev. B 2, 2887 (1970).
[24]D. E. Ellis and G. S. Painter, in *Computational Methods in Band Theory,* edited by P. M. Marcus, J. F. Janak, and A. R. Williams (Plenum, New York, 1971), pp. 271 and 276.
[25]R. S. Mulliken, J. Chem. Phys. 23, 1833 (1955); 23, 1841 (1955).
[26]D. E. Ellis, G. A. Benesh, and E. Byrom, Phys. Rev. B 16, 3308 (1977).
[27]D. E. Ellis, G. A. Benesh, and E. Byrom, Phys. Rev. B 20, 1198 (1979).
[28]U. von Barth and L. Hedin, J. Phys. C 5, 1629 (1972).
[29]K. H. Johnson, D. D. Vvedensky, and R. P. Messmer, Phys. Rev. B 19, 1519 (1979).
[30]R. Podloucky, R. Zeller, and P. H. Dederichs, Phys. Rev. B 22, 5777 (1980); R. Zeller and P. H. Dederichs, Phys. Rev. Lett. 42, 1713 (1979).
[31]V. I. Anisimov, V. A. Gubanov, D. E. Ellis, and E. Z. Kurmaev, J. Phys. F 11, 405 (1981).